Pakistan
Journal of Biological Sciences

Synthesis of Magnetic Al/Au Nanoparticles by Co-Reduction of Au^{3+} and Al^{3+} Metal Salts

M. Gilaki

Department of Chemistry, University of Mazanderan, Babolsar, Iran

Abstract: In current study, it reported the synthesis of water soluble; monos disperse Al/Au bimetallic nanoparticles with a middling length of 7 nm. Synthesis engages concurrent reduction of Al^{3+} and Au^{3+} in water to give way bimetallic nanoparticles. The elemental content of Al is 1.5%. Nanoparticles display ferromagnetic performance as deliberate by SQUID. These particles can be effortlessly conjugated to thiolated DNA, as confirmation by mobility shifts in agarose gel electrophoresis. Nanoparticles heat in solution to temperatures above 40°C, representative appropriateness for hyperthermia.

Key words: DNA, bimetallic, ferromagnetic, bioconjugation, TEM

INTRODUCTION

Magnetic nanoparticles have been exploited in a broad diversity of biological request such as sensing devices (Chemla *et al.*, 2000; Perez *et al.*, 2002), sarcoma conduct by hyperthermia (Berry *et al.*, 2003), drug delivery (Kawashima, 2010), separation (Wang *et al.*, 2001) and imaging *in vivo* (Högemann *et al.*, 2002). Current novelty in magnetic sensors has established an immense contract of attention as counterparts to conservative glowing labels. All of these purposes necessitate magnetic nanoparticles that can be effortlessly conjugated with biomolecules. Classically aluminum oxide nanoparticles are engaged, as there has been a huge contract of recent progress in their synthesis. Homogeneous and crystalline nanoparticles of aluminum oxide and a variety of other magnetic materials can now be regularly accomplished (Sun *et al.*, 2004; Zhihua *et al.*, 2006; Puntes *et al.*, 2001). Nevertheless, synthesis is mainly in organic solvents, so nanoparticles are capped with a hydrophobic ligand that create water solubility demanding. Hydrophilicity is essential for conjugation to biomolecules. In order to move organically synthesized magnetic nanoparticles from organic solvents into an aqueous phase, amphiphilic ligands (Pablo and Nicols, 2010) or custody molecules (Wang *et al.*, 2003; Josephson *et al.*, 2001) have been used productively to protect the hydrophobicity of the nanoparticle. However, one would like to take benefit of the well-developed chemistry of Au bioconjugation, as Au nanoparticles have been successfully linked to DNA (Zanchet *et al.*, 2001) and a diversity of proteins (McMillan *et al.*, 2002). In addition, functional groups on DNA are extensively commercially available and many proteins contain cysteine remains appropriate for conjugation. Decontamination method such as gel electrophoresis have previously been established and optimized for Au nanoparticle-protein and DNA conjugates (Jhaveri *et al.*, 2004). Subjects such as non-specific adsorption of the biomolecule on Au nanoparticles have been considered and can be chemically controlled (Park *et al.*, 2004). Additionally, Au nanoparticles and nanostructures have attractive optical properties that allow numerous sensing and control purpose (Hirsch *et al.*, 2003). So, combining the properties of gold with magnetic materials would be beneficial. It demonstrated here the synthesis of Al/Au bimetallic nanoparticles by at the same time reducing Al^{3+} and Au^{3+} in water, resulting in water soluble nanoparticles. Since these nanoparticles are mainly composed of Au, they can with no trouble be conjugated to DNA via standard Au-thiol chemistry. SQUID measurements point out that they are magnetic. These Al/Au nanoparticles have potential for use in biological applications that require magnetic nanoparticles, such as hyperthermia (Shinkai *et al.*, 1999).

MATERIALS AND METHODS

All experiment has conducted at Chemistry Laboratory, Islamic Azad University, South Tehran branche (2009). For Al/Au Nanoparticle Synthesis: The metal solution was composed of 3 mL of 1% HAuCl$_4$ (Merk Co.) with 6 mL 1% AlCl$_3$ in 231 mL H$_2$O (1:7 molar ratio). The reducing solution was composed of 12 mL of 1% sodium citrate (Merk Co.) and 3.0 mL of 1% tannic acid (Merk Co.) with an equal volume of 25 mM sodium carbonate (Merk Co.) in H$_2$O made up to 60 mL volume. The metal solution and reducing solution were heated separately to 50°C. The metal solution darkened from light yellow-orange color to profound orange. At 50°C the reducing solution was added to the metal solution with vigorous stirring. Upon addition of the reducing solution,

the reaction immediately turned a deep wine red color. The solution was stirred at 50°C for 10 min and allowed to cool to room temperature. Excess bis (p-sulphonatophenyl) phenylphosphine dihydrate, dipotassium salt (BPS) was added and allowed to ligand exchange on the nanoparticle surface for 16 h. Nanocrystals were precipitated with excess sodium chloride and collected by centrifugation. The supernatant was orange-brown in color, most likely due to unreacted aluminum. Solids were collected and washed thoroughly with water to remove excess salt. Solids were redissolved in a minimal amount of water and the concentrated solution was run through a 1.5% agarose gel in 0.5X TBE at a field strength of 4.36 V cm^{-1}. The red nanoparticle band was cut out of the gel and the nanoparticles were extracted by centrifugation through a spin filter (Corning). Finally, the nanoparticle solution was precipitated with ethanol and stored as solid before use. The nanoparticles were stable in solution for several weeks and UV-vis absorption showed no change in Plasmon position or width, suggesting that there was no nanoparticle aggregation or degradation. TEM. Nanoparticles were imaged by TEM on a JEOL 2010 FEG Analytical Electron Microscope (Fig. 1a, b). Samples were

deposited from aqueous solution onto ultrathin holey carbon coated copper grids (Ted Pella). Size distributions were measured directly from TEM images from at least 100 nanoparticles. STEM. Samples were imaged by a HB603 Scanning Transmission Electron Microscope as shown in Fig. 2a and b as well as Fig. 3a and b. Sample preparation was identical to that for TEM. SQUID. Superconducting quantum interference device (SQUID) magnetometry was performed on a Quantum Design DC Magnetic Property Measurement System. Al/Au nanoparticles were in powder form, prepared as above, of approximately 6 mg. M-H curves were measured from 30 kOe to-30 kOe. Bioconjugation. Al/Au nanoparticles were conjugated to 15 nucleotide single stranded DNA that were modified on the 5 ends with C6 thiols (Proligo, Inc.), sequence 5'ATATA TATAT GCGCG. Conjugation was done in 0.5X PBS buffer by combining appropriate volumes of 1.86 μM DNA and 0.52 μM Al/Au to give 5:1, 10:1 and 20:1 molar ratios of DNA to particles. Samples were run through agarose gels under conditions described above in synthesis (Fig. 4). Hyperthermia. Approximately 100 μL of a 3.7 μM solution of the nanoparticles was placed in an alternating magnetic field at a frequency of 40 MHz and
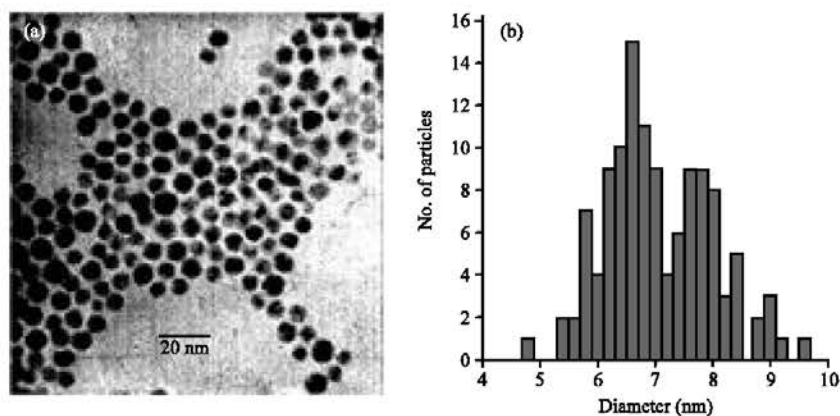

Fig. 1: (a)TEM of Al/Au nanoparticles and (b) corresponding histogram, d = 7.0 ±0.96 nm
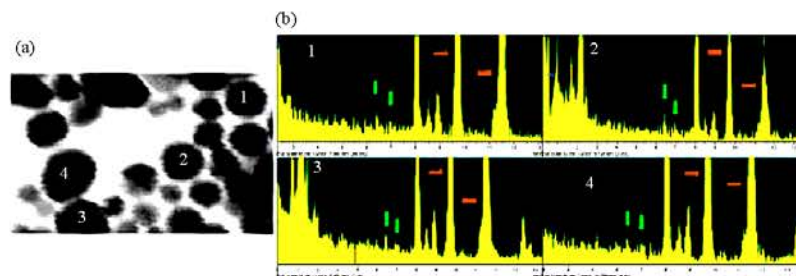

Fig. 2: (a) STEM of Al/Au nanoparticles and (b) elemental analysis of the four particles labeled in a. ↓ arrows indicated Al peaks, → arrows indicate Au peaks
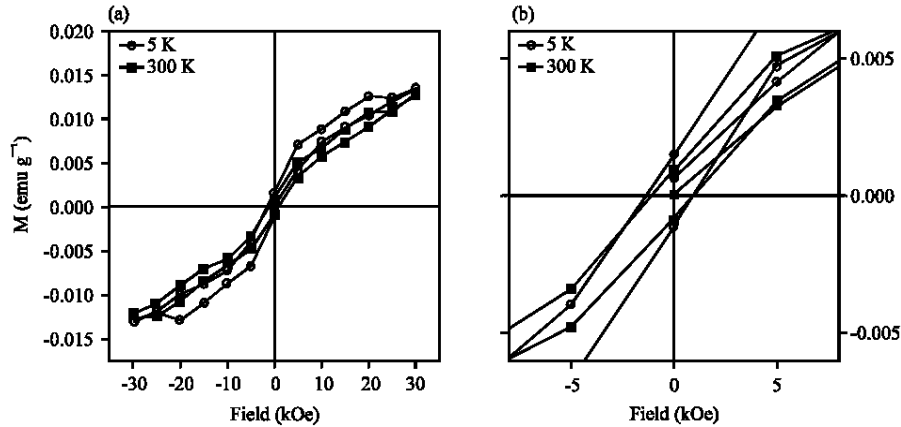
Fig. 3: Magnetization curves of Al/Au nanoparticles taken by SQUID magnetometry at 5 K (circles) and 300 K (squares)
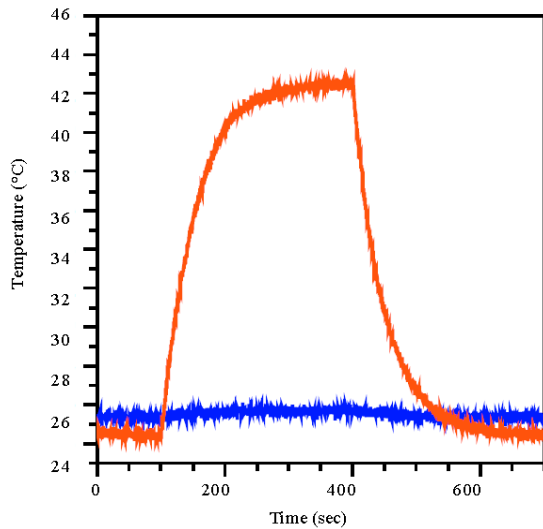

Fig. 4: Hyperthermia of a 3.7 µM solution of Al/Au nanoparticles (curve line) and a control solution of BPS ligand (193 µM, horizental line). A 40 MHz field of 100 A/m field strength is applied and the temperature of the solution is measured

a field strength of approximately 100 A/m. Control solutions of the BPS ligand were also measured. The concentration of the BPS ligand in the Al/Au NP solution was determined by removing all of the ligand from the nanoparticles by incubation with 1 mM of mercaptohexanol (Sigma Aldrich) overnight, which displaces the BPS from the NP surface. The Nanoparticles were then removed from the solution by centrifugation. The concentration of BPS in the supernatant was determined by optical absorption at 265 nm, which determines that there are approximately 50 BPS ligands present on a NP surface.

RESULTS AND DISCUSSION

Production of Al/Au nanoparticles by using a concurrent reduction of Au^{3+} and Al^{3+} consequences in well separated and mono disperse nanoparticles, as confirmation by the TEM image and corresponding histogram (Fig. 1). Size analysis discloses an average length of 7±1 nm. For comparison, a pure Au nanoparticle synthesis under identical conditions yields 8nm particles, indicating that presence of the Al^{3+} affects nanoparticle growth.

The atomic composition of the Al/Au particles was probed by STEM on large fields of particles (data not shown) and on individual particles (Fig. 2). STEM measurements of the four numbered particles are shown. Area analysis of Al and Au peaks indicate an average elemental content of 1.5% Al in the particles. Whole field elemental analysis indicates Al content of 1.8%. Scans of background areas containing no particles yield no Al signal and only Au scattering signal levels. These data indicate that Al is incorporated into the Au nanopaticles, rather than existing as separate particles.

Further, evidence of Al incorporation into particles was obtained by x-ray mapping of nanoparticles.

The magnetic properties of the particles were probed by SQUID in powder form, Robinson *et al.* (2005) prepared as above, of approximately 6 mg. M-H curves were measured at 5 and 300 K from 30 to -30 kOe (Fig. 3). The nanoparticles display typical ferromagnetic behavior, with a finite hysteresis at both 5 K (circles) and 300 K (squares). These measurement adapted with the results of similar works. Andrew (2002) and Mary-Catherine (2008) measured coecivities were Hc = 1388 Oe at 5 K and 1080 Oe at 300 K.

Nanoparticle-DNA conjugates are stable in buffer, enabling the use of gel electrophoresis for separation. In

addition, their strong plasmon resonance facilitates visualization in the gel as shown by the dark red color of the bands. The bands of the bioconjugated Al/Au nanoparticles are retarded relative to that of the plain Al/Au nanoparticles. The decrease in mobility is due to the formation of a bond between the DNA and the nanoparticle (Zanchet *et al.*, 2001; Jhaveri *et al.*, 2004). This shows that the same chemistry used for Au nanoparticles can be applied to Al/Au nanoparticles, enabling their use in a wide variety of biological applications alternating magnetic field (Aubin *et al.*, 2005; Parak *et al.*, 2003; Pablo and Nicols, 2010). The heating profile of Al/Au nanoparticles was measured by application of an alternating magnetic field at 40 MHz and 100 A/m. The nanoparticle solution increased in temperature to approximately 43°C (Fig. 4, curve line), a sufficient temperature to allow the use of Al/Au nanoparticles for hyperthermia applications. A solution of the surface ligand BPS of the same concentration (1.93 ×10-4 M) was then placed in the alternating magnetic field under identical conditions to those used for the Al/Au nanoparticles. The BPS solution shows negligible temperature increases (Fig. 4, horizontal line) with a VT ≤0.5°C, demonstrating that the heating observed is not due to the surface ligand or solvent, but the nanoparticles themselves (Cao *et al.*, 2002; Högemann *et al.*, 2002).

CONCLUSION

It showed that co-reduction of Au^{3+} and Al^{3+} metal salts produces Al/Au bimetallic nanoparticles. These particles acquire the constructive properties of Au nanoparticles for biological request such as effortlessness of conjugation to DNA and compatibility with agarose gel electrophoresis. Al/Au nanoparticles exhibit ferromagnetism and can be animated in an alternating magnetic field, demonstrating appropriateness for magnetic field heating claims.

REFERENCES

Andrew, T., 2002. Preparation of gold nanoparticle-DNA conjugates. Curr. Protocols Nucl. Acid Chem., Unit No.12.2. 10.1002/0471142700.nc1202s09

Aubin, M.E. and D.G. Morales, 2005. Labeling ribonuclease S with a 3 nm Au nanoparticle by two-step assembly. Hamad-Schifferli K Nano Lett., 5: 519-522.

Berry, C.C. and A.S.G. Curtis, 2003. The smithsonian/NASA astrophysics data system. J. Phys. D Applied Phys., 36: R198-R206.

Cao, Y.C., R. Jin and A.C. Mirkin, 2002. Nanoparticles with raman spectroscopic fingerprints for DNA and RNA detection. Science, 297: 1536-1540.

Chemla, Y.R., H.L. Grossman, Y. Poon, R. McDermott, R. Steven, M.D. Alper and J. Clarke, 2000. Ultrasensitive magnetic biosensor for homogeneous immunoassay. Proc. Natl. Acad. Sci. USA., 97: 14268-14272.

Hirsch, L.R., R.J. Stafford, J.A. Bankson, S.R. Sershen and B. Rivera *et al.*, 2003. Nanoshell-mediated near-infrared thermal therapy of tumors under magnetic resonance guidance Proc. Natl. Acad. Sci. USA., 100: 13549-13554.

Högemann, D., V. Ntziachristos, L. Josephson and R. Weissleder, 2002. Imaging for evaluating targeted nanoparticle probes. Bioconjugate Chem., 13: 116-121.

Jhaveri, S.D., E.E. Foos, D.A. Lowy, E.L. Chan, A.W. Snow and M.G. Ancona, 2004. Solation and characterization of trioxyethylene-encapsulated gold nanoclusters functionalized with a single DNA strand. Nano Lett., 4: 737-740.

Josephson, L., J.M. Perez and R. Weissleder, 2001. Magnetic nanosensors for the detection of oligonucleotide sequences. Angew. Chem. Int. Ed. Engl., 40: 3204-3206.

Kawashima, Y., 2010. Nanoparticles Enhance therapeutic efficiency by selectively increased local drug dose in experimental colitis in rats. J. Pharmacol. Exp. Therapeutics, 315: 196-202.

Mary-Catherine, B., 2008. Inhibition of HIV fusion with multivalent gold nanoparticles. Am. Chem. Soc., 130: 6896-6897.

McMillan, R.A., C.D. Paavola, J. Howard, S.L. Chan, N.J. Zaluzec and J.D. Trent, 2002. Conformation ordered nanoparticle arrays formed on engineered chaperonin protein templates. Nat. Mater., 1: 247-252.

Pablo, G. and P. Nicols, 2010. Controlled synthesis of iron oxide nanoparticles over a wide size range. Langmuir, 26: 5843-5847.

Parak, W.J., T. Pellegrino, C.M. Micheel, D. Gerion, S.C. Williams and A.P. Alivisatos, 2003. Conformation of oligonucleotides attached to gold nanocrystals probed by gel electrophoresis. Nano Lett., 3: 33-36.

Park, S., K.A. Brown and K. Hamad- Schifferli, 2004. Changes in oligonucleotide conformation on nanoparticle surfaces by modification with mercaptohexanol. Nano Lett., 4: 1925-1929.

Perez, J.M., L. Josephson, T. OLoughlin, D. Hogemann and R. Weissleder, 2002. Magnetic relaxation switches capable of sensing molecular interactions. Nat. Biotechnol., 20: 816-820.

Puntes, V.F., K.M. Krishnan and A.P. Alivisatos, 2001. Colloidal nanocrystal shape and size control: The case of cobalt. Science, 291: 2115-2117.

Robinson, D.B., H.H.J. Persson, H. Zeng, G. Li, N. Pourmand, S. Sun and S.X. Wang, 2005. DNA-functionalized MFe2O4 (M=Fe, Co, Mn) nanoparticles and their hybridization to DNA-functionalized surfaces. Langmuir, 21: 3096-3103.

Shinkai, M., M. Yanase, M. Suzuki, H. Honda, T. Wakabayashi, J. Yoshida and T. Kobayashi, 1999. Intracellular hyperthermia for cancer using magnetic cationic liposomes. J. Magn. Magn. Mater, 194: 176-184.

Sun, S., H. Zeng, D.B. Robinson, S. Raoux, P.M. Rice, S.X. Wang and G. Li, 2004. Monodisperse MFe2O4 (M = Fe, Co, Mn) nanoparticles. J. Am. Chem. Soc., 126: 273-279.

Wang, J., A.N. Kawde, A. Erdem and M. Salazar, 2001. Magnetic bead-based label-free electrochemical detection of DNA hybridization. The Analyst, 126: 2020-2024.

Wang, Y., J.F. Wong, X. Teng, X.Z. Lin and H. Yang, 2003. Pulling nanoparticles into water: Phase transfer of oleic acid stabilized monodisperse nanoparticles into aqueous solutions of á–cyclodextrin. Nano Lett., 3: 1555-1559.

Zanchet, D., C.M. Micheel, W.J. Parak, D. Gerion and A.P. Alivisatos, 2001. Electrophoretic isolation of discrete Au nanocrystal/DNA conjugates. Nano Lett., 1: 32-35.

Zhihua, Z., L. Meihua, X. Hairuo and C. Wee-Shong, 2006. Shape-controlled synthesis of zinc oxide: A simple method for the preparation of metal oxide nanocrystals in non-aqueous medium. Chem. A Eur. J., 13: 632-638.